

## MEASUREMENT OF ADHESION STRENGTH OF BONDS USING NONLINEAR ACOUSTICS

S. U. Fassbender and W. Arnold  
Fraunhofer Institute for Non-Destructive Testing  
University, Bldg. 37  
D-66123 Saarbruecken, Germany

### INTRODUCTION

It is well known that the nonlinear elastic behavior of solids modulates transmitting ultrasonic wave [1]. Higher harmonics of the fundamental frequency are generated, especially second harmonics describing the deviation from the linear elastic behavior of the solid. Some effects were also observed in ultrasonic velocity [2] and transmission of ultrasound [3] due to the nonlinear elastic behavior of interfaces. In general, reduced bonding of joined materials causes a strong nonlinear elastic behavior [4]. We exploit this for the observation of the modulation of the ultrasonic wave at interfaces [5,6]. There exist several models based on a macroscopic description of the interface restoring forces using for example the extended Hooke's Law [7] or nonlinear spring relations [3,8].

### THEORY

The adhesion strength of joined materials is dominantly described by the behavior of their interfaces, usually the weakest parts of the composite. An interface is created by two surfaces separated by a certain distance, normally in the Å region. The binding energy of the interface is given by a potential, its derivative being the restoring force  $F(a)$  of the interface (Fig. 1), i.e. the force necessary to separate the surfaces of the interface by a certain distance. The interface binding force is the maximum value  $F_{\max}$  of the restoring force. This description is valid for chemical and physical as well as other bindings [9,10]. Many technical interfaces can be described by one of these two binding types, like interfaces of composites, grain boundaries, closed cracks, etc.. The distance  $a_0$  between the two surfaces of an ideal interface where the binding energy is maximal is the equilibrium position of the interface. Due to boundary conditions such as residual stresses, different thermal expansion coefficients and impurities, the real distance  $a_i$  between the surfaces of the interface can be larger than  $a_0$  (Fig. 1). We call this position  $a_i$  the resting position. According to figure 1 the resting position is in a non-equilibrium state, stabilized by the boundary conditions. This kind of interface is regarded to be poorly bonded. In terms of the restoring force, a poorly bonded interface can be described by a shift of the origin of the coordinate from  $a_0$  to  $a_i$  along the  $F(a)$ -curve where the shifted coordinates are given by the change in the distance between the surfaces of the interface and the force generated by the boundary conditions. It is obvious that the binding force of the poorly bonded interface is smaller than that of the well bonded interface. This holds also for the gradient of the restoring force.

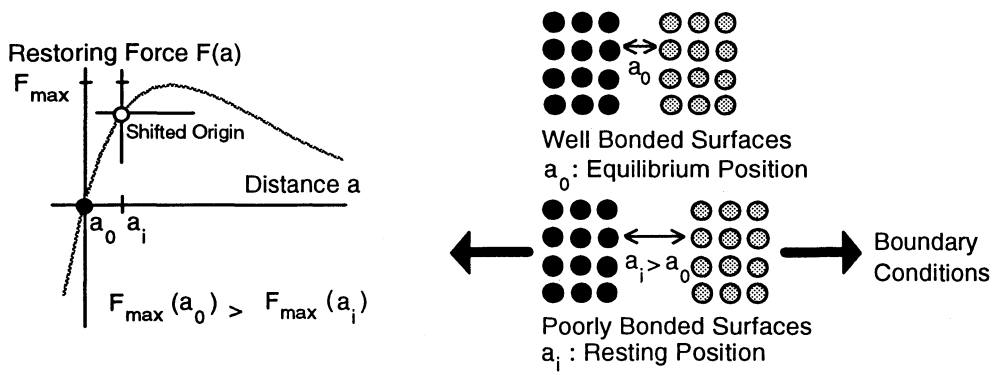


Figure 1. Definition of the restoring force of well and poorly bonded interfaces.

The interface can be displaced from its resting by mechanical loading resulting in a restoring force  $F_{re}$  equal to the external mechanical loading force  $F_{ext}$ . For large displacements  $F_{ext}$  approaches the binding force  $F_{max}$ . This effect can be used to characterize the interface binding force nondestructively. An ultrasonic wave is used as mechanical load.

For plane surfaces of the interface, the microscopic description of the restoring force for one type of chemical bonding, the metallic binding is given by [9,10]:

$$F(a) = 2E_{ad} \frac{a}{l_{sc}^2} \exp\left(\frac{-a}{l_{sc}}\right) \quad (1)$$

Here,  $E_{ad}$  is the surface energy, and  $l_{sc}$  is a screening or scaling length. Weak bonds result in an increase of the amplitude of the incident ultrasonic wave at the interface. This can easily be seen, considering the reflection coefficient for the particle velocity  $v_1$  of the ultrasonic wave in the case of linear transmission through the interface [11]:

$$v_1 = -\frac{1}{Z_{01}} \left[ P\left(t - \frac{x}{v_0}\right) - \Gamma P\left(t + \frac{x}{v_0}\right) \right] \quad (2)$$

Here,  $P$  is the incident pulse,  $\Gamma = (Z_{02} - Z_{01}) / (Z_{02} + Z_{01})$  is the reflection coefficient and  $Z_{01,02}$  are the acoustic impedances of the adjacent media. For a completely disbonded interface  $Z_{02} = 0$ , hence  $\Gamma = -1$  doubling the particle velocity at the interface and the displacement. However, the strain  $S_0$  at the interface will be zero. The mechanical displacement  $a(t)$  of the interface due to the incident ultrasonic wave with frequency  $\omega_1$ , amplitude  $u_0$  and the wave number  $k$  depends on the restoring force at the interface [12].  $a(t)$  can be written as:

$$a(t) = a_i + a_i S_0 \sin(\omega_1 t - k_1 x) \quad (3)$$

By substituting Eq. 3 into Eq. 1, the resulting transfer function  $F(a_i + S_0)$  becomes a Fourier-integral without an analytic solution known to us. Therefore, we expanded Eq. 1 as a Taylor series around the resting position  $a_i$  yielding a summation of the amplitudes  $A_i$  of the fundamental frequencies and their higher harmonics [13]. The magnitudes of the amplitudes  $A_i$  of the higher harmonics depend on the nonlinearity of the gradient of the restoring force and on the displacement of the interface caused by the incident ultrasonic wave. For increasing  $u_0$  the nonlinear part of the restoring force  $F_{re}$  becomes dominant, resulting in an increasing influence of the amplitudes of the higher harmonics  $A_i$  ( $i > 1$ ) in  $F[a_i + S_0]$ . Also due to the stronger elastic nonlinearity of poorly bonded interfaces, higher harmonics were

generated for smaller amplitudes of the incident ultrasonic wave. Other potentials than the one of Eq. 1 will lead in principle to similar nonlinearities. In composites for example, the restoring force of the interface has to be taken into account as well as the restoring forces of the joined materials (fiber, matrix). Usually, the interfaces having the weakest restoring forces result in the strongest modulation of the transmitting ultrasonic wave.

## EXPERIMENTAL ARRANGEMENT

The experimental arrangement consists of the components shown schematically in Fig. 2. The measurements are done in transmission. The sending probe is excited by a narrowband ultrasound burst of about 30 oscillations. The transmitted ultrasonic wave is received by a broadband probe. The electrical signal is transferred to an oscilloscope and passes a Fourier transformation to determine the amplitudes  $A_i$  of the higher harmonics as a function of the ultrasonic amplitude  $u_0$ . The transfer functions of the sending as well as of the receiving probe were taken into account. However, the DC-part  $A_0$  of the transmitted ultrasonic wave cannot be determined. For the presented samples the frequency of the incident ultrasonic wave was 2 MHz. The amplitude of the ultrasonic wave determined from sound-field calculations [14] was in the Å-region. By variation of  $u_0$  and summation of the respective  $A_i$ , the restoring force curve can be measured nondestructively up to its maximum on a relative scale [6]. Despite the relative scale, the quality of the composite can be compared for a set of samples with differently bonded interfaces of the same type. The absolute binding force for a set of samples can be obtained by destructive calibration techniques [5].

## EXPERIMENTAL RESULTS AND DISCUSSION

Reinforcement of composites can be achieved by the embedding of high modulus fibers in a ductile matrix material. The nature of the binding mechanism between fiber and matrix can be due to mechanical friction, physical or chemical bonds in which mechanical friction produces the weakest bonds, and chemical bonds the strongest bonds. Composites contain many interfaces between fibers and matrix. Each of these interfaces contributes to the nonlinear elastic behavior of the composite.

### Mechanically Loaded C/C-Composites

Due to mechanical or thermal loading, joined structures of carbon reinforced carbon composites were damaged. We have investigated 21 C/C samples manufactured by Sigr. The samples were cyclicly loaded with a rate of 20 kPa/s and an amplitude of 15 MPa. The stress cycle frequency was varied between 0, 0.1, 1, and 10 Hz [15]. As a break off criterium, a transverse elongation of 20  $\mu\text{m}$  was chosen. During loading at the interfaces microdelaminations were generated which can be described as an increase in the averaged distance between the surfaces of all inner interfaces. With an increasing number of microdelaminations the mechanical strength of the composite decreases.

Measurements were done in the direction of the fibers and perpendicular to the woven fabric (Fig. 3). The measured compliance of the composites indicates the damage due to mechanical loading. Here, the compliance is the ratio of the transverse strain to the applied stress (Fig. 4). Two different regions can be distinguished: I. a linear increase of the measured compliance with increasing load. Here, microcracks were generated inside of the composite. II. starting at a load of approximately 80 MPa, the measured compliance is increasing strongly caused by macrodelaminations [15]. To separate the influence of both effects on the nondestructive measurement results, we have plotted the maximum of the measured restoring force (the measure of the adhesion strength of the composite) as a function of cyclic frequency, measured compliance (influence of macrodelaminations) (Fig. 5),

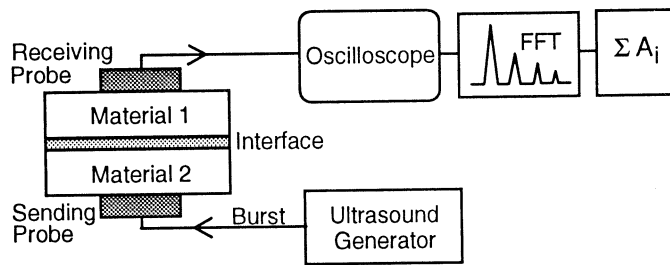


Figure 2. Experimental arrangement.

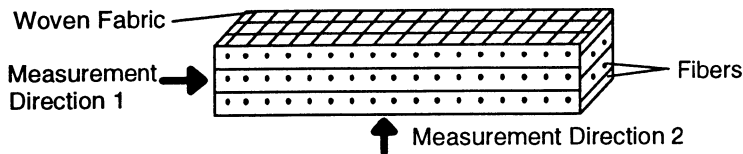


Fig. 3: Geometry and measurement directions of the investigated samples.

and the compliance extrapolated from region I to the maximal applied load (influence of microcracks) (Fig. 6). Despite the scattering of the data due to the inhomogeneity of the composites, a decrease of the adhesion strength with increasing cyclic frequency is found. There is no dependance on the measured compliance (region II Fig. 4) and therefore no influence of macrodelaminations on the modulation of the transmitting ultrasonic wave. However, there is a strong dependance between the extrapolated compliance (region I Fig. 4) and the nondestructively measured strength of the composites explained by the strong nonlinear behavior of the microcracks modulating the ultrasonic wave. Due to the friction between fiber and matrix, this effect is stronger in the measurement direction along the woven fabric than in the direction perpendicular. Therefore, using nonlinear acoustics one can determine the fatigue of components caused by microcracks.

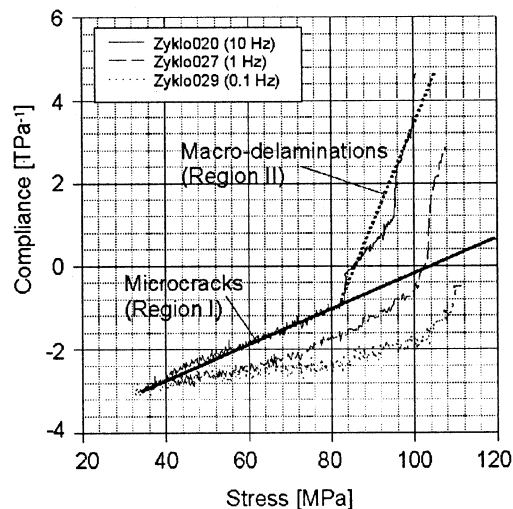


Fig. 4: Measured compliance of cyclically loaded C/C-composites. Here, the compliance is the ratio of the transverse strain to the applied stress [15]. Two regions can be distinguished caused by I. microcracks and II. macrodelaminations.

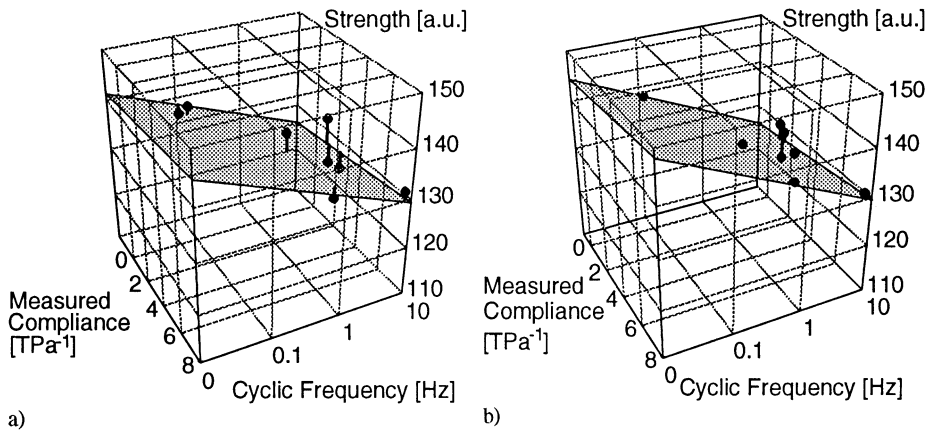


Fig. 5: Nondestructively measured adhesion strength of C/C-composites as a function of cyclic frequency and measured compliance. Propagation directions of the ultrasonic waves were a) along the fibers and b) perpendicular to the woven fabric. Despite the scattering of the measurement data, a decrease of the adhesion strength with increasing cyclic frequency is found. There is no dependence on the measured compliance [15]. For clearness a best fit is shown (shaded area). Bars indicate the position of the data points relative to the best fit.

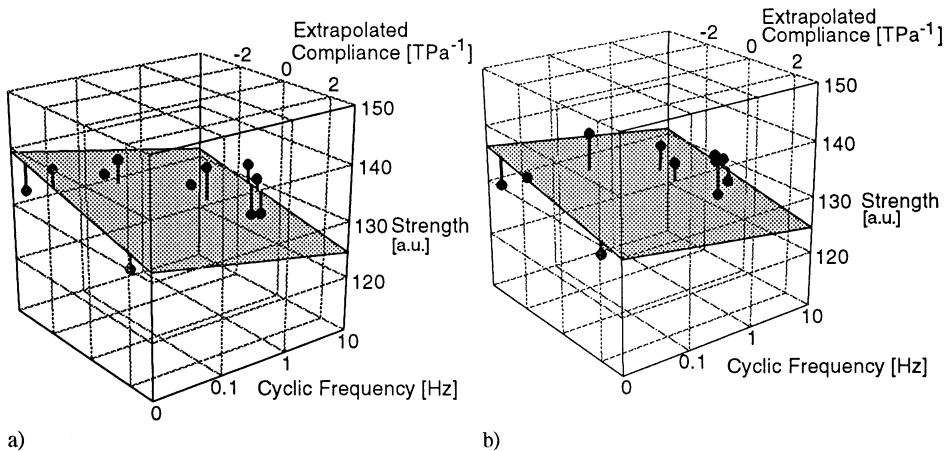


Fig. 6: Nondestructively measured adhesion strength of C/C composites as a function of cyclic frequency and compliance was extrapolated to find the maximal loading force. Propagation directions of the ultrasonic waves were a) along the fibers and b) perpendicular to the woven fabric. Despite the scattering of the measurement data, a decrease of the adhesion strength with increasing frequency and increasing compliance could be found [16]. For clearness a best fit is plotted in the diagrams (shaded area). Bars are a guide to indicate their position relative to the best fit.

### Mixing of Two Waves at an Interface

Using high power excitation, the nonlinearities of the electronic components like the ultrasonic transducers have to be carefully considered. The nonlinear elastic behavior of the interface can be separated from the nonlinearities of the electronic components and possibly other effects [1] using two incident ultrasonic waves of frequencies  $\omega_1$  and  $\omega_2$ . Here, the generated mixing frequencies (sum frequency  $\omega_1 + \omega_2$  and the difference frequency  $\omega_1 - \omega_2$ ) are caused by the nonlinear elastic behavior of the interface only. Based on the considerations outlined above, the amplitude of the mixing frequencies is a measure for the adhesion

strength of the interface. As a boundary condition necessary to generate mixing frequencies due to the non-linear transmission of ultrasound, the projected wavelengths  $\lambda_s$  of the two incident ultrasonic waves have to match at an interface. Hence, due to Snell's law the incident angles  $\theta_1$  and  $\theta_2$  of the two ultrasonic waves is given by:

$$\lambda_s = \frac{\lambda_1}{\sin \theta_1} = \frac{\lambda_2}{\sin \theta_2} \quad (4)$$

The angle of emergence  $\theta_i$  of the waves with wavelength  $\lambda_s$  and with mixing frequencies is also given by Eq. (4). Experiments were done on nickel coated aluminum consisting of a 100  $\mu\text{m}$  thick nickel layer on a 6 mm thick aluminum substrat. Ni is contracted when exposed to a magnetic field because it is magnetostrictive. The contraction generates a small gap between the nickel layer and the aluminum substrat resulting in a reduction of the adhesion strength of the interface entailing an increase of the nonlinear elastic behavior of the interface. Thus different adhesion strengths can be simulated by variation of the magnetic field intensity. The experimental set-up is shown in Fig. 7. The sample is placed in a variable magnetic field of an electromagnet. Two narrowband ultrasonic transducers with frequencies  $\omega_1 = 5$  MHz and  $\omega_2 = 7$  MHz having incident angles  $45^\circ$  and  $30^\circ$ , respectively, are placed in such a way that the two incident ultrasonic waves coincide at the interface. The transmitted ultrasonic wave is detected by a broadband ultrasonic transducer which is coupled by water. The detection angle of the receiving transducer can be varied and the received signal is transformed in its frequency spectrum.

The frequency spectrum measured under a detection angle of  $4^\circ$  is shown in Fig. 8. Besides the fundamental frequencies  $\omega_1 = 5$  MHz and  $\omega_2 = 7$  MHz of the incident ultrasonic waves and their higher harmonics (10 and 14 MHz), other frequencies could be detected which can be identified as mixing frequencies, especially the difference frequency ( $\omega_2 - \omega_1$ ) at 2 MHz, the sum frequency ( $\omega_1 + \omega_2$ ) at 12 MHz, and the sum and difference frequencies of higher harmonics ( $3\omega_2 - \omega_1$ ) at 16 MHz and ( $\omega_1 + 2\omega_2$ ) at 19 MHz. Beside the central ray of the ultrasonic beam, the edge rays also contribute to the generation of mixing frequencies. Therefore, there exists a range of angle of emergence for the mixing frequencies which could be taken into account in Eq.4 by a corresponding spatial Fourier transform of the incident ultrasonic beams. Furthermore, the magnetic field intensity was varied in steps of 20 A/cm resulting in an increasing contraction of the nickel layer corresponding to a strain of 0,  $-1.1 \cdot 10^{-5}$  and  $-1.7 \cdot 10^{-5}$ , respectively [16]. For the investigated detection angles the amplitude of the mixing frequency increases with increasing magnetic field intensity (Fig. 9). This is a clear indication that the nonlinear transmission through the gap is the cause of the ultrasonic waves at the mixing frequencies

## CONCLUSION

It was demonstrated that the study of nonlinear transmission of ultrasound is useful to characterize C/C-composites during the optimization process of fabrication parameters, as well as for fatigue life predictions of mechanical loaded C/C-composites. Furthermore, the non-linear transmission of ultrasound was demonstrated by mixing two waves of different frequencies at a Nickel-aluminium interface.

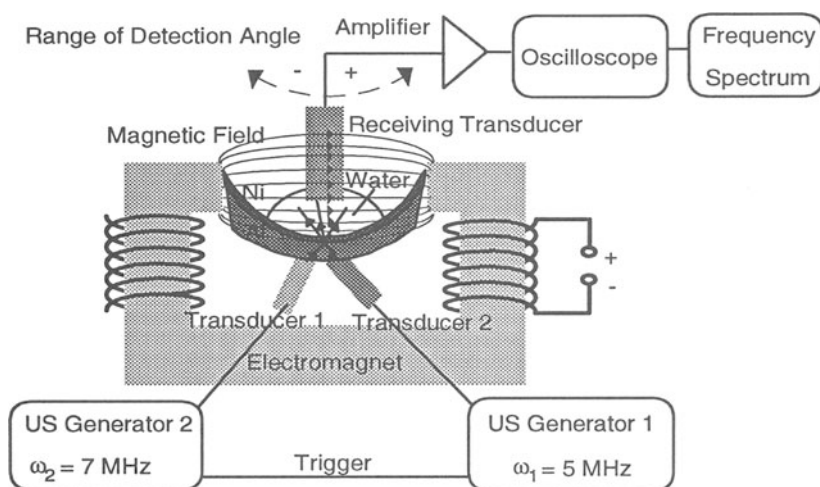


Fig. 7: Experimental set-up. The sample, nickel coated aluminum, is placed in an electro-magnet. By varying the magnetic field intensity, the nickel layer contracts and different adhesion strength can be simulated.

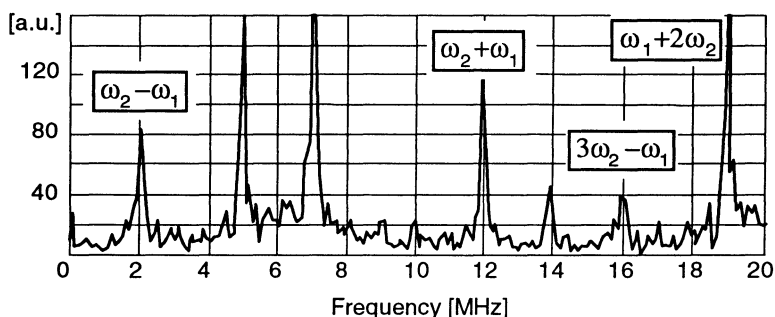


Fig. 8: Frequency spectrum of the measured signal. Detection angle:  $4^\circ$ . Beside the fundamental frequencies  $\omega_1$  (5 MHz) and  $\omega_2$  (7 MHz) and their higher harmonics other frequencies could be detected which can be identified as mixing frequencies.

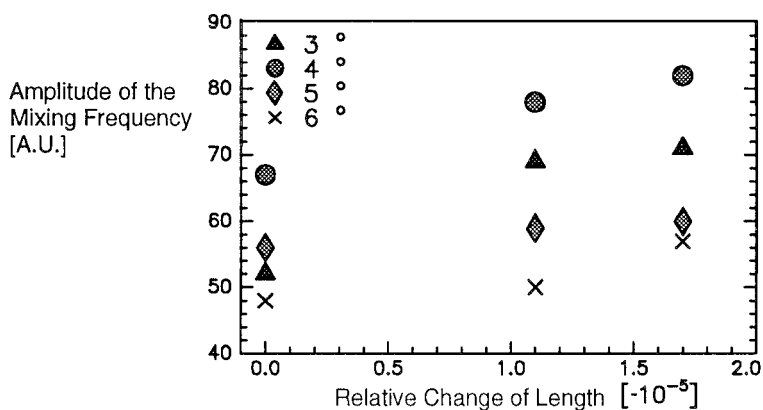


Fig. 9: Measured amplitude of  $(\omega_2 - \omega_1) = 2 \text{ MHz}$  for different angles as a function of the relative change of length caused by different magnetic field intensities.

## ACKNOWLEDGEMENT

This work was supported by the German Science Foundation in the „Schwerpunktprogramm höchsttemperaturbeständige Leichtbauwerkstoffe“. It is a pleasure to thank K. Kromp, W. Lins, and H. Peterlik of the University of Vienna, Austria, for close collaboration and fruitful discussions. Furthermore, we benefitted from many discussions with K.J Hüttinger and K.M Beinborn, University of Karlsruhe, on various aspects of composite materials

## REFERENCES

1. M.A. Breazeale and J. Philip, Physical Acoustics XVII, Eds. W.P.Mason and R.N. Thurston, **XVII**; **1** (1984)
2. H. Mohrbacher, D. Lee, E. Schneider, and K. Salama, *Review of Progress in QNDE* **10B**, Eds. D.O. Thompson and D.E. Chimenti, Plenum Press N.Y., 1821 (1991)
3. I.Y. Solodov, A.F. Asainov, K.S. Len, Ultrasonics **31**, 91 (1993)
4. J. D. Achenbach and O. K. Parikh, *Review of Progress in QNDE* **10B**, Eds. D.O. Thompson and D. E. Chimenti, Plenum Press N. Y., 1837 (1991)
5. S. Pangraz and W. Arnold, *Review of Progress in QNDE* **13B**, Eds. D.O. Thompson and D.E. Chimenti, Plenum Press N. Y., 1995 (1994)
6. S.U. Faßbender, M. Kröning, and W. Arnold, Proc. 8th Int. Symp. Non-Destr. Mat.Characterization, Prague 1995, to be published
7. L. Adler and P. B. Nagy, *Review of Progress in QNDE* **10B**, Eds. D.O. Thompson and D. E. Chimenti, Plenum Press, N. Y., 1813 (1991)
8. S. Hirose and M. Kitahara, *Review of Progress in QNDE* **11A**, Eds. D. O. Thompson and D. E. Chimenti, Plenum Press, N. Y., 33 (1992)
9. J. H. Rose, J.R. Smith, F. Guinea, J. Ferrante, Phys. Rev. **B29**, 2963 (1984)
10. J. Ferrante, J.R. Smith, Phys. Rev. **B31**, 3427 (1985)
11. G. Kino, *Acoustic Waves*, Prentice Hall, Englewood Cliffs (1987)
12. J.D. Achenbach and O. Parikh, J. Adhes. and Sci. Tech. **5**, 601 (1991)
13. S. Pangraz, PhD-Thesis, Technical Faculty, University of Saarbrücken and Fraunhofer IzfP report #950117-TW, unpublished
14. J. Krautkrämer and H. Krautkrämer, *Ultrasonic Testing of Materials*, 3rd edition Springer Press, New York, 62 (1983)
15. W. Lins, W. Bernauer, S. Fassbender, H. Peterlik, W. Arnold, K. Kromp, Fortschrittsberichte der Deutschen Keramischen Gesellschaft, 1995, to be published
16. Landolt-Börnstein, *Technik*, **IV**, part 2b, 6th edition, Springer Press Berlin/ Göttingen/Heidelberg, 568(1964)